Mehran University Research Journal of Engineering and Technology

https://doi.org/10.22581/muet1982.2202.05

2022, 41(3) 43-53

Fractional order modelling and robust multi-model intelligent controllers' synthesis for ACP1000 nuclear power plant

Arshad Habib Malik [a,*], Aftab Ahmed Memon [b], Feroza Arshad [c]

[a] *Maintenance and Technical Training Division, Pakistan Atomic Energy Commission, Chashma Punjab Pakistan*

[b] *Department of Telecommunication Engineering, Mehran University of Engineering and Technology, Jamshoro Sindh Pakistan*

[c] *Computer Development Division, Pakistan Atomic Energy Commission, Karachi Sindh Pakistan*

[*] Corresponding author: Arshad Habib Malik, Email: mastermind_arshad@yahoo.com

Received: 18 September 2021, Accepted: 25 February 2022, Published: 01 July 2022

KEYWORDS

Fractional Order Modelling

Intelligent Controller

ACP1000

Nuclear Power Plant

ABSTRACT

In this research work, a third generation Pressurized Water Reactor (PWR) type Nuclear Power Plant (NPP) of 1100 MWe rating called Advanced Chinese PWR (ACP1000) NPP is adopted. The research and development work is mainly encompassed of addition of third steam generator loop, hybrid programming platforms, fractional order modular modelling and intelligent controllers. The ACP1000 NPP is comprised of primary loop, secondary loop and balance of plant (BOP). The ACP1000 nonlinear dynamics is precisely modelled with greater efficiency using fractional order differential equations. The entire plant is modelled into eighteen modules in a fractional order framework in Visual Basic (VB) environment. The eighteen modules are governed by nine controllers. Controllers are configured in a fashion of an adaptive neuro-fuzzy inference system (ANFIS). An innovative multi input single output (MISO) ANFIS virtual instrument (VI) is designed for training and configuring controllers in LabVIEW. The developed MISO ANFIS VI in combination is implemented for multi-input multi output (MIMO) ANFIS controllers in parallel computing framework. The variable transfer between fractional order multi- modular framework in VB (FO-MMF-VB) and robust intelligent ANFIS controllers in LabVIEW (RI-ANFIS-LV) is established in client server configuration and system exec VI for calling external code in VB. This hybrid programming framework of Visual Basic and LabVIEW is actually a development of LabVIEW Visual Basic Integration (LabVb) Toolkit used to evaluate the closed loop transient performance of ACP1000 nuclear power plant. Various parameters are simulated for dynamic transient simulations under load manoeuvring from 100% power to 50% power. The results are analysed and validated against benchmark design data and Preliminary Safety Analysis Report (PSAR). All the results are within the protection systems design limits under normal operating conditions.

1. Introduction

This research work is based on dynamic modelling, simulation and analysis of ACP-1000 Nuclear Power Plant using a new proposed state-of-the-art nuclear power plant dynamics code known as Robust Intelligent Control Oriented Fractional Order Multi-Model ACP-1000 Nuclear Power Plant Dynamics (RIC-FOMM-ACP1000-NPPD) Code. RIC-FOMM-ACP1000-NPPD code is developed and it deals with different scenarios and a case study is presented in this research work for ramp load reduction from 100% full power to 50% at a rate of 10% per min.

In ACP1000 type Nuclear Power Plant, the plant is broadly classified into three major categories of loops, called primary loop (PL), secondary loop (SL) and balance of plant (BOP). The plant monitoring, control and protection systems are implemented on Distributed Control System (DCS). All the control logics are hard coded by the vendor. Therefore, in this research work, a comprehensive model based plant operation and control is formulated in an intelligent and hybrid computational framework using plant design and operational data.

Technical data and literature is explored for comprehensive modelling and control design of ACP1000 nuclear power plant. The plant layout, configuration of plant systems and safety aspects of ACP1000 nuclear power plant has been reviewed in detail in [1-2]. Since ACP1000 is a three loop nuclear power plant, therefore, the modelling and control aspects have been thoroughly investigated in [3]. The special design aspects of nuclear reactor core and load following control strategy have been established in [4]. The reactor power controller design with special emphasis on turbine load has been evaluated in detail in [5]. The primary loop (PL) has been thoroughly modelled for Russian PWR for controller design purposes in [6]. Similarly, the primary loop of PWR has been modelled and simulated in [7]. The two loop whole AP1000 type PWR nuclear power plant has been modelled and conventional controllers have been configured for grid transient studies in [8]. The secondary loop (SL) of PWR type nuclear power plant has been modelled with special emphasis on steam turbine, feed water pump, ejector and condenser in [9]. A robust fractional order PID controller has been designed for dynamic mechatronic system in [10]. The research has been explored for fractional order vibratory system with synthesis of LQR controller in [11]. A research work has been further extended for fractional order interval systems with uncertain dynamics in [12]. A research is explored for fractional order nuclear reactor kinetic studies in [13] and further extended with feedbacks for reactor dynamics in [14].

Some literature has been reviewed in which Adaptive Neuro-Fuzzy Inference System (ANFIS) has been adopted as controller in [15]. A research has been explored in which ANFIS controller has been used for single phase full bridge inverter in [16]. An investigation has been made in [17] for the optimization of ANFIS controller using ant colony algorithm. In [18], different algorithms such as grid portioning, subtractive clustering, fuzzy C-mean clustering, and context based fuzzy C-mean clustering methods have been investigated for the optimization of ANFIS controllers.

Our proposed methodology is one step ahead in this direction to develop a fractional order multi-model modular framework of three loop ACP1000 using primary loop, secondary loop and an addition of balance of plant (BOP) with ANFIS based intelligent MISO and MIMO controllers. The entire closed loop model of ACP1000 nuclear power plant is a hybrid platform of Visual Basic and LabVIEW with a special scheme of variable transfer of plant and controller parameters as compared to other third generation PWR type nuclear plants reported in [8-9].

2. Modelling Of ACP1000 Nuclear Power Plant

There are total 374 systems in ACP1000 nuclear power plant but in this research work some major systems are considered for dynamic modelling. The control oriented modelling approach is structured in eighteen modules and nine controllers. The layout of selected modules and controllers is shown in Fig. 1.

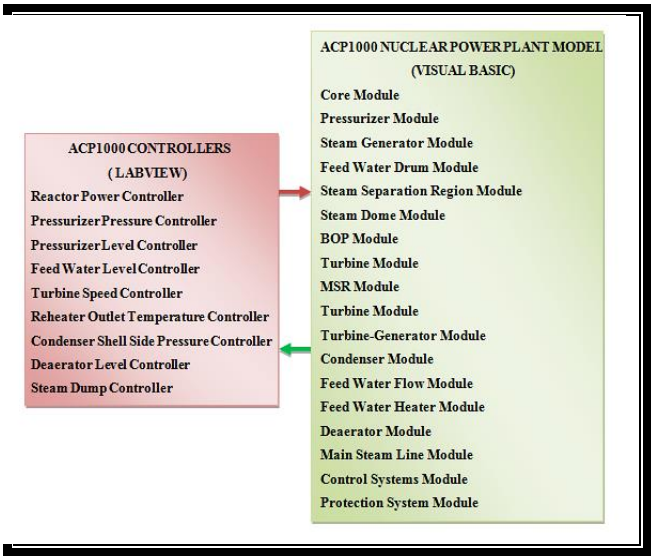

Fig. 1. Layout of ACP1000 modules and controllers

In Fig. 1, the modelling of ACP1000 encompasses the nuclear power plant equipment, systems and broadly

the plant loops. The primary loop mainly focuses the reactor core, pressuriser and steam generator while the secondary loop mainly focuses on steam turbine, moisture separator, deaerator and condenser.

The controllers associated with primary and secondary loops are considered in this research work. The protection systems are meant to actuate beyond the controller design safe limits and to keep the plant within the design safety margins. The coupling of FO-MMF-VB and RI-ANFIS-LV is shown in Fig. 2.

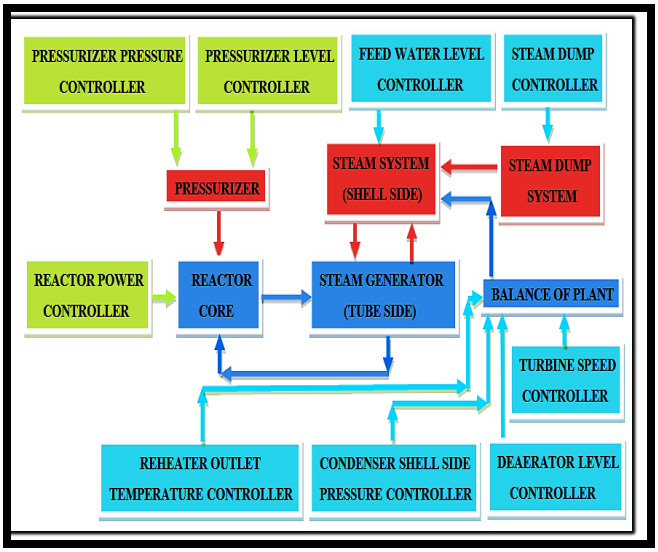

Fig. 2. Coupling of FO-MMF-VB and RI-ANFIS-LV

3. Fractional Order Modelling

Fractional-order modelling is useful in studying the anomalous behaviour of nuclear power plant dynamics. Fractional order derivatives and integrals are basically mathematical representations for describing power law memory phenomena. Fractional order models are used to describe better time response with more robust performance and better optimization.

3.1 Fractional Order Modelling of Primary Loop

If η_i are the variational fractional orders associated with time domain differential operators $D_t^{\eta_i}$ and space domain integral operators $I_x^{\eta_i}$ then these operators are used to model primary and secondary loop systems.

The one group coupled point reactor kinetics of ACP1000 reactor core [3] can be modelled as follows.

$$D_t^{\eta_1} P_N(t) = \frac{(\rho_{RC}-\beta)}{l} P_N(t) + \lambda C(t) \quad (1)$$

$$D_t^{\eta_2} C(t) = \frac{\beta}{l} P_N(t) - \lambda C(t) \quad (2)$$

Where $P_N(t)$, β, l, λ and ρ_{RC} are the neutron flux power or reactor power, delayed neutron fraction, neutron lifetime, decay constant and reactivity respectively.

The reactor thermal power of ACP1000 reactor core [3] can be modelled as follows.

$$P_{th}(t) = \frac{V_{Core}\Sigma_f \varphi_{thermal}}{(3.12\times10^{10})} \quad (3)$$

Where V_{Core}, Σ_f and $\varphi_{thermal}$ are the reactor core volume, macroscopic fission cross section and reactor thermal flux respectively.

The core reactivity [8] is computed as follows.

$$\rho_{RC}(t) = \rho_0(t) + \alpha_F(T_F(t) - T_{F_0}) + \alpha_C(T_C(t) - T_{C_0}) + \alpha_{Xe}(X_e(t) - X_{e_0}) + \rho_{CR}(t) + \rho_B(t) \quad (4)$$

Where ρ_0, ρ_{CR}, ρ_B, α_F, α_C, α_{Xe}, T_F, T_C and Xe are initial reactivity, control rod reactivity, boron reactivity, fuel temperature coefficient of reactivity, coolant temperature coefficient of reactivity, Xenon coefficient of reactivity, fuel temperature, coolant temperature and Xenon concentration respectively.

The average temperature of the reactor coolant [6] is given as follows.

$$T_{AV}(t) = \frac{T_{CL}(t)+T_{HL}(t)}{2} \quad (5)$$

Where T_{CL} and T_{HL} are cold leg and hot leg temperatures respectively.

The non-equilibrium three region mass flow rate dynamics of steam region, main liquid region and surge flow region of pressuriser of ACP1000 [8] can be modelled as follows.

$$D_t^{\eta_3} m_1(t) = \dot{m}_{A1} + \dot{m}_{A2} - \dot{m}_{A3} - \dot{m}_{A4} - \dot{m}_{A5} - \dot{m}_{A6} - \dot{m}_{A7} \quad (6)$$

$$D_t^{\eta_4} m_2(t) = \dot{m}_{B1} + \dot{m}_{B2} + \dot{m}_{B3} + \dot{m}_{B4} + \dot{m}_{A3} + \dot{m}_{A4} + \dot{m}_{A5} - \dot{m}_{A1} - \dot{m}_{A2} \quad (7)$$

$$D_t^{\eta_5} m_3(t) = \dot{m}_{C1} - \dot{m}_{B4} \quad (8)$$

Where m_1, m_2, m_3 and $\dot{m}(.)$ are the mass of coolant in steam region, main liquid region, surge flow region in pressuriser and different mass flow rates associated with three regions respectively.

The pressuriser pressure dynamic model [8] is given as follows.

$$D_t^{\eta_6} P \frac{A}{B_{Pr}} \quad (9)$$

Where,

$$A = \left[m_1 \frac{\partial^{\eta_6} v_1}{\partial h^{\eta_6}} \frac{d^{\eta_6} h_1}{dt^{\eta_6}} + v_1 D_t^{\eta_3} m_1(t) + m_2 \frac{\partial^{\eta_6} v_2}{\partial h^{\eta_6}} \frac{d^{\eta_6} h_2}{dt^{\eta_6}} + v_2 D_t^{\eta_3} m_2(t) + m_3 \frac{\partial^{\eta_6} v_3}{\partial h^{\eta_6}} \frac{d^{\eta_6} h_3}{dt^{\eta_6}} + v_3 D_t^{\eta_3} m_3(t) \right]$$

$$B = \begin{pmatrix} m_1 \frac{\partial^{\eta_6} v_1}{\partial P_{Pr}^{\eta_6} \frac{\partial^{\eta_6} v_2}{\partial P_{Pr_3}^{\eta_6} \frac{\partial^{\eta_6} v_3}{\partial P_{Pr}^{\eta_6}}}} \end{pmatrix},$$

And, $v_1(.), h_1(.), v_2(.), h_2(.), v_3(.), h_3(.)$ and P_{Pr} are specific volume and enthalpy of the in steam region, specific volume and enthalpy of main liquid region, specific volume and enthalpy of surge flow region and pressuriser pressure respectively.

The three region dynamics of sub-cooled region, boiling region and steam region of steam generator of ACP1000 [8] can be modelled in terms of temperature and pressure dynamics as follows.

$$D_t^{\eta_7} T_P(t) = \frac{2m_C - h_P}{2c_{c_{SG}}} T_{HL}(t) - \frac{2m_C + h_P}{2c_{c_{SG}}} T_P(t) + \frac{h_P}{c_{c_{SG}}} T_U(t) \quad (10)$$

$$D_t^{\eta_8} T_{CL}(t) = \frac{2m_C - h_P}{2c_{c_{SG}}} T_{HL}(t) - \frac{2m_C + h_P}{2c_{c_{SG}}} T_P(t) + \frac{h_P}{c_{c_{SG}}} T_U(t) \quad (11)$$

$$D_t^{\eta_9} T_U(t) = \frac{h_P}{4c_{c_U}} T_{HL}(t) + \frac{h_P}{2c_{c_U}} T_P(t) + \frac{h_P}{4c_{c_U}} T_{CL}(t) - \frac{(h_P + h_S)}{c_{c_U}} T_U(t) + \frac{h_S}{c_{c_U}} C_F(P_S(t)) \quad (12)$$

$$D_t^{\eta_{10}} P_S(t) = \frac{h_S}{\tau_{P_S}} T_U(t) - \frac{h_S}{\tau_{P_S}} C_F(P_S(t)) + \frac{Q_S(h_{F_W} - h_{Steam})}{\tau_{P_S}} \quad (13)$$

Where $m_C = \dot{m}_C c_{P_C}, \dot{m}_C, c_{P_C}, h_P, h_S, c_{c_{SG}}, c_{c_U}, C_F(P_S(t)), \tau_{P_S}, T_P, T_U, h_{F_W}, h_{Steam}, P_S$ and Q_S are mass flow rate of coolant, specific heat capacity of coolant at constant pressure, the fluid pressure, specific enthalpy of fluid, heat transfer coefficient between coolant and U-tube, heat transfer coefficient between U-tube and steam, specific heat capacity of coolant in steam generator, specific heat capacity of coolant in U-tube, conversion factor between steam pressure and steam temperature as a function of steam pressure, time constant of steam pressure, primary coolant temperature, U-tube metal temperature, enthalpy of feed water at inlet temperature, enthalpy of steam, steam pressure and steam flow respectively.

3.2 Fractional Order Modelling of Secondary Loop with Emphasis on Balance of Plant

Now, in this section, fractional order model of secondary loop of ACP1000 nuclear power plant is modelled with emphasis on balance of plant (BOP). BOP mainly focuses on steam turbine, moisture separator, deaerator and condenser.

The steam turbine of ACP1000 consists of one high pressure (HP) turbine, one intermediate pressure (IP) turbine and three low pressure (LP) turbines. The steam control valve opening demand is given as follows.

$$\tau_{CV} D_t^{\eta_{11}} X_{Open} = K_{CV} X_{Open}^{Ref} \quad (14)$$

Where τ_{CV}, K_{CV}, X_{Open} and X_{Open}^{Ref} are the time constant, gain, control valve opening position and reference control valve opening position respectively.

The total steam turbine power at *n*-th stage is given as follows.

$$P_T = \sum_{j=1,k=HP,IP,LP}^{n=n_{HP}+n_{IP}+n_{LP}} P_{j,k} \quad (15)$$

Where *j*, *k* and $P_{j,k}$ are number of stages, type of turbine and *j*-th stage power of *k*-th turbine respectively.

The speed of steam turbine coupled with generator on common shaft [9] is given as follows.

$$\tau_{Inertia} D_t^{\eta_{12}} w(t) = T_{Mech} - T_{Elect} \quad (16)$$

Where $\tau_{Interia}, T_{Mech}$ and T_{Elect} are the inertial time constant, mechanical torque and electrical torque respectively.

The moisture separator and reheater are lumped together for modelling purposes and re-heater outlet temperature [9] is given as follows.

$$T_{Out}^{Re\,heater}(t) = \left(\alpha_{Temp-1}^{Re\,heater} + \alpha_{Temp-2}^{Re\,heater} \frac{P_S^{Re\,heater-In}(t)}{P_S^{Re\,heater-In}} \right) T_S^{Re\,heater-Out} \quad (17)$$

Where $\alpha_{Temp-1}^{Re\,heater}$, $\alpha_{Temp-2}^{Re\,heater}$, $P_S^{Re\,heater-In}$, $T_S^{Re\,heater-Out}$ and $P_S^{Re\,heater-In}(t)$ are temperature coefficient-1, of re-heater, temperature coefficient-2 of re-heater, nominal steam pressure at re-heater inlet, nominal steam temperature at re-heater outlet and steam pressure at re-heater inlet respectively.

The tube side temperature dynamics of condenser [9] is given as follows.

$$D_t^{\eta_{13}} T_{Out}^{Coolant}(t) = \frac{Q_{Coolant}}{m_{Coolant} c_p^{Coolant}} - \dot{m}_{Coolant} \frac{(T_{Out}^{Coolant}(t) - T^{Coolant}(t))}{m_{Coolant}} \quad (18)$$

Where $Q_{Coolant}$ is the heat transfer from shell side steam to tube side coolant.

The shell side steam dynamics of condenser is given as follows.

$$D_t^{\eta_{14}} m_{Steam}(t) = \dot{m}_{Out}^{LP/SD} - \dot{m}_{Coolant} \quad (19)$$

Where $\dot{m}_{Out}^{LP/SD}$ is the low pressure or steam dump mass flow rate.

The steam pressure dynamics at shell side of condenser is given as follows.

$$D_t^{\eta_{15}} P_S(t) = \frac{(T_{Coolant}+273)}{V_{Steam}} D_t^{\eta_{14}} m_{Steam}(t) \quad (20)$$

The feed water flow dynamics [9] is computed by following fractional order integro-differential equation.

$$D_t^{\eta_{16}} m_{FW}(t) I^{\eta_{16}}(A_{FW}(z)) = (P_{Deaerator}(t) + \Delta P_{MFP}(t) - P_S(t)) - I^{\eta_{16}}(g\rho_{FW}(z)) - \Delta P_{MFCV}(t) - \Delta P_{MFCHKV}(t) - \Delta P_{MFIV}(t) \quad (21)$$

Where $\Delta P_{MFP}(t)$, $\Delta P_{MFCV}(t)$, $\Delta P_{MFCHKV}(t)$ and $\Delta P_{MFIV}(t)$ are pressure drops across main feed water pump, main feed water control valve, main feed water check valve and main feed water isolation valve respectively.

The extraction steam from HP, IP and LP steam turbines is used to identify the dynamics of feed water heater as follows.

$$m_{FWH} c_p^{FWH} D_t^{\eta_{17}} T_{Out}^{FWH}(t) = \sum_k \dot{m}_{In}^{FWH} h_{In}^{FWH} - \sum_k \dot{m}_{Out}^{FWH} h_{Out}^{FWH} \quad (22)$$

The deaerator is provided to control the chemistry to prevent from corrosion. The dynamics of steam and water regions [9] can be modelled as follows.

$$D_t^{\eta_{18}} m_{Deaerator}^{Steam}(t) = \sum \dot{m}_{Deaerator}^{Steam} \quad (23)$$

$$D_t^{\eta_{18}}(m_{Deaerator}^{Steam}(t) h_{Deaerator}^{Steam}(t)) - D_t^{\eta_{18}}(P_{Deaerator}^{Steam}(t) V_{Deaerator}^{Steam}(t)) + m_{Deaerator}^{Steam} c_{P_{Deaerator}}^{Steam} D_t^{\eta_{18}} T_{Deaerator}(t) = \sum \dot{m}_{Deaerator}^{Steam} h_{Deaerator}^{Steam} \quad (24)$$

$$D_t^{\eta_{19}} m_{Deaerator}^{Water}(t) = \sum \dot{m}_{Deaerator}^{Water} \quad (25)$$

The dynamics of steam flow can be modelled as follows.

$$Q_S = C_{QP} \frac{P_S}{P_S^{Rated}} \quad (26)$$

Where C_{QP} is the conversion constant.

4. Intelligent ANFIS Controllers

In Section-3, detailed multi-model modelling of ACP1000 nuclear power plant is completed. Now, in this section, multi-model based ANFIS controllers are designed for reactor power controller, pressuriser level controller, pressuriser pressure controller, feed water level controller, turbine speed controller, reheater outlet temperature controller, condenser shell side pressure controller, deaerator level controller and steam dump controller. A state-of-the-art-new virtual instrument (VI) is designed for MISO ANFIS controller in LabVIEW, which is reused in combination for MIMO ANFIS controllers in parallel soft computing frameworks.

4.1 MISO ANFIS Controller

In this research work, a Takagi and Sugeno's rule based ANFIS controller is adopted as reference controller known as ANFIS Type-3 controller [16]. ANFIS Type-3 controller is adaptive controller optimized by Fuzzy Clustering Mean (FCM) algorithm that finds the optimal clustering of data. It is structured in Multi-Input and Single Output (MISO) fashion with output as first order linear equation. The parameters of membership functions are computed and output of controller is returned by using least square estimation and backpropagation algorithms against the inputs and output of ANFIS controller depicting like or mapping conventional controller. It is a hybrid learning algorithm. The set of total parameters is divided into two set of parameters; one is known as set of premise parameters while other is known as set of consequence parameters. Therefore, in hybrid learning algorithm, the set of premise parameters is computed with gradient decent while set of consequence parameters is calculated with least square estimation. For the reasoning used in MISO ANFIS Type-3 controller is difficult to assign appropriate linguistic terms to the consequence part which is a non-fuzzy function of the input variables, to minimize these disadvantages, simplified IF-THEN rules are used. The structure of ANFIS controller is shown in Fig. 3.

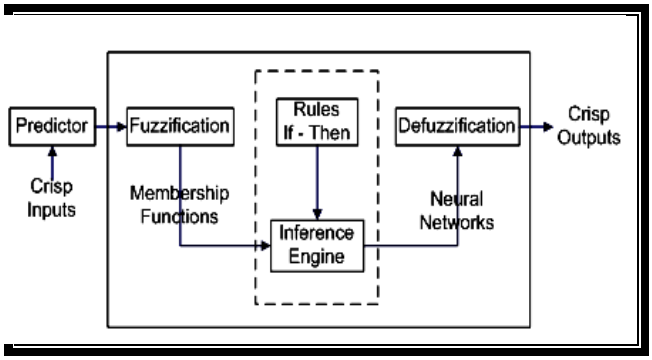

Fig. 3. Structure of ANFIS

The framework of two inputs and one output five layer MISO ANFIS controller is shown in Fig. 4.

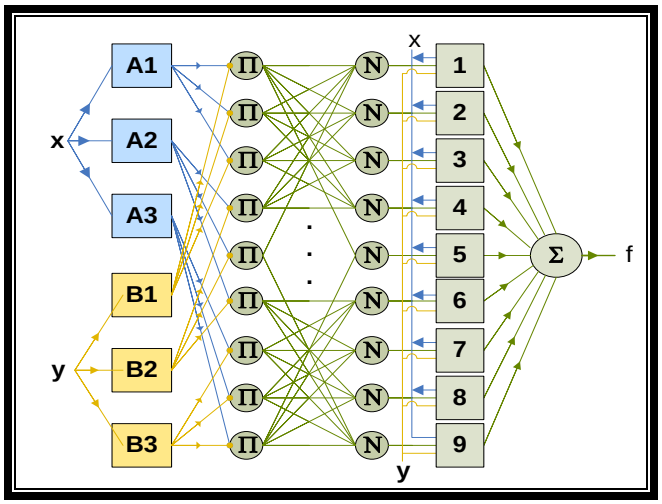

Fig. 4. Framework of MISO ANFIS controller

Layer-1 to layer-5 are designed to represent the "IF Part", "Rules Part", "T-Norm Part", "THEN Part" and "Output Part" respectively. The transition from layer-1 to layer-5 in which nonlinear premise parameters are passed from fixed to least square estimator as linear consequent parameters is called forward pass while the transition from layer-5 to layer-1 in which linear consequent parameters are passed from fixed to gradient decent as nonlinear premise parameters is called backward pass. Consequent parameters are adaptive in nature. A_l and B_l are the linguistic labels (l = 1, 2,…., L) associated with layer-1. Label Π is the product output of layer-2. Label N is the firing strength associated with layer-3. Layer-4 is associated with R-rules. Layer-5 is the summation (Σ) of all signals meant for the computation of overall output of controller.

The output of MISO ANFIS controller $K = f$ is basically the output of 5th layer given as follows.

$$K = f = \frac{\sum_{l=1}^{L}\left(\frac{(\mu A_l(x)\mu B_l(y))(p_l x+q_l y+r_l)}{\sum_{l=1}^{L}(\mu A_l(x)\mu B_l(y))}\right)}{\sum_{l=1}^{L}(\mu A_l(x)\mu B_l(y))} \quad (27)$$

Where the membership functions of A_l and B_l are described by bell-shaped functions [17], given as follows.

$$\mu A_l(x) = \frac{1}{1+\left\{\left(\frac{(x-c_l)}{a_l}\right)^2\right\}b_l} \quad (28)$$

$$\mu B_l(y) = \frac{1}{1+\left\{\left(\frac{(y-c_l)}{a_l}\right)^2\right\}b_l} \quad (29)$$

Where a_l, b_l and $c_l$the parameters of that define the form of bell.

4.2 Optimization of ANFIS Controllers

The optimization of ANFIS controllers is carried out using Fuzzy Clustering Mean (FCM) algorithm in LabVIEW. The FCM is basically adopted the optimal clustering of input data $D = \{d_1, d_2,\ldots\ldots,d_m\}$. Firstly, the input data is partitioned into c number of clusters $P(D) = Un\ (dm)$, where $Un\ (dm)$ are the fuzzy subsets such that satisfying the following conditions [18].

$$\sum_{n=1}^{c} U_n(d_m) = 1 \quad (30)$$

$$0 < \sum_{p=1}^{m} U_n(d_m) < m \quad (31)$$

The number of clusters that the Fuzzy Clustering Mean (FCM) can pop up is as below.

$$c = [2, m-1] \quad (32)$$

The vector point corresponding to the n-th cluster is given as follows.

$$q_n = \frac{\sum_{r=1}^{m}[U_n(d_m)]^s d_m}{\sum_{r=1}^{m}[U_n(d_m)]^s} \quad (33)$$

The partition clusters of FCM are updated using Euclidean norm [18] as follows.

$$U_n(d_m) = \left[\sum_{u=1}^{c}\left(\frac{\|(d_m-q_n)\|^2}{\|(d_m-q_u)\|^2}\right)^{\frac{1}{s-1}}\right]^{-1} \quad (34)$$

Where s >1.

The performance index of FCM [18] is given as follows.

$$J_s(P(D)) = \sum_{r=1}^{m}\sum_{n=1}^{c}[U_n(d_m)]^s \|(d_m - q_n)\|^2 \quad (35)$$

The mean square error (MSE) for MISO ANFIS controller is given as follows.

$$MSE = \frac{1}{m}\sum_{r=1}^{m}(K-\widehat{K})^2 \quad (36)$$

5. Variable Transfer between ACP1000 Model and ANFIS Controllers

5.1 Hybrid Programming Platforms

The variable transfer between ACP1000 model (FO-MMF-VB) and ANIFIS controllers (RI-ANFIS-LV) is accomplished via hybrid programming platforms of Visual Basic and LabVIEW.

5.2 Scheme of Parametric Transfer

The scheme of variable transfer between FO-MMF-VB and RI-ANFIS-LV is shown in Fig. 5 through a comprehensive block diagram.

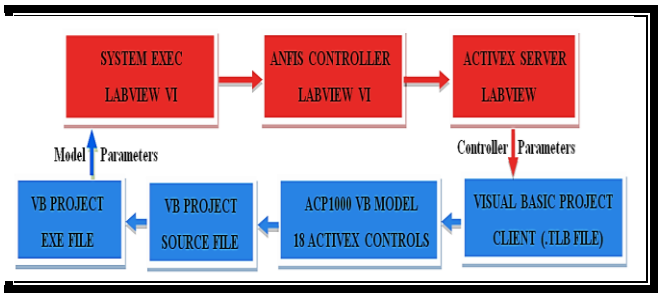

Fig. 5. Interfacing scheme of LabVIEW with visual basic

6. Optimization of Closed Loop Framework

The optimization of ACP1000 model and ANFIS controllers is carried out in closed loop framework as shown in Fig. 6.

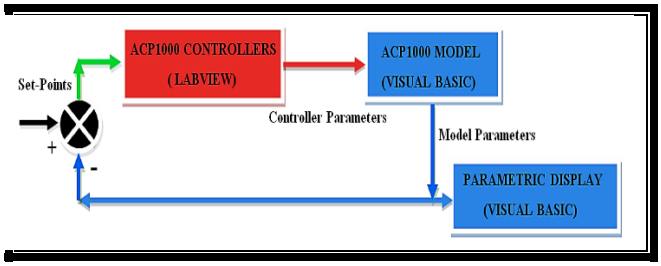

Fig. 6. Closed loop coupled interfaced configuration

All the parametric dynamic trends are visualized on Visual Basic Display. For the process of optimization, two key parameters are selected as Power Core Thermal and Power Turbine Load. When these two parameters follows exactly or near around one another then it ensures the entire closed loop framework is set at an optimal conditions of design parameters.

The process of optimization under different dynamic transient conditions is carried out and the best optimal performance is shown in Fig. 7.

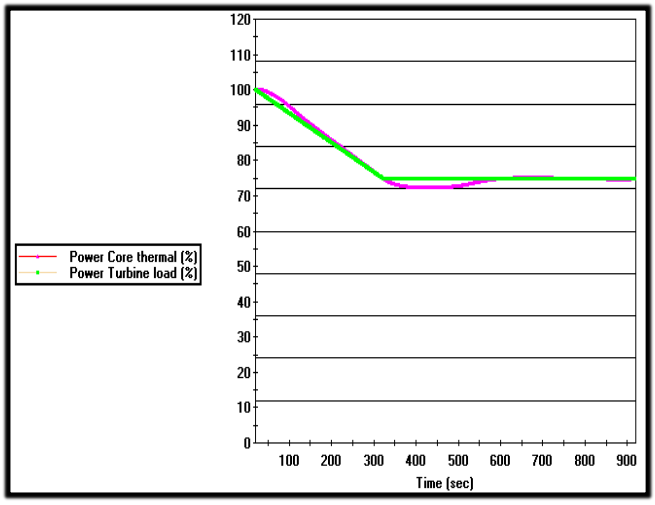

Fig. 7. Optimization of closed loop performance for power reduction from 100% to 75% at a rate of 5%/min

7. Evaluation of Design Parameters of ACP1000 Model and ANFIS Controllers

The optimized parameters of FO-MMF-VB are tabulated in Table 1.

Table 1

Design parameters of FO-MMF-VB

Parameter	Value	Parameter	Value
η_1	0.981	η_{11}	0.952
η_2	0.963	η_{12}	0.973
η_3	0.954	η_{13}	0.994
η_4	0.975	η_{14}	0.985
η_5	0.946	η_{15}	0.956
η_6	0.967	η_{16}	0.986
η_7	0.998	η_{17}	0.924
η_8	0.935	η_{18}	0.946
η_9	0.957	η_{19}	0.983
η_{10}	0.928		

The optimized values of design parameters in Table 1 are achieved using applied Fractional Variational Calculus (FVC) based on variational virtual work coupled with the Lagrange multiplier technique. The design configuration of multi-model RI-ANFIS-LV controllers is tabulated in Table 2.

Table 2

Design Configuration of RI-ANFIS-LV Controllers

Parameter	Value
Number of RI-ANFIS Controllers	9
Total Premise Parameters for Three MISO ANFIS Controllers	54
Total Premise Parameters for Six MIMO ANFIS Controllers	216
Total Consequent Parameters for Three MISO ANFIS Controllers	27
Total Consequent Parameters for Six MIMO ANFIS Controllers	108
Total Parameters for Three MISO ANFIS Controllers	81
Total Parameters for Six MIMO ANFIS Controllers	324

The optimized design parameters in Table 2 are achieved using Fuzzy Clustering Mean (FCM) algorithm. All parameters are achieved based on mean square error minimization algorithm. The optimized parameters of RI-ANFIS-LV are tabulated in Table 3.

Table 3

Design Parameters of Multi-Model RI-ANFIS-LV Controllers

Parameter	Value
Number of Clusters for RI-ANFIS-1	7
Number of Clusters for RI-ANFIS-2	5
Number of Clusters for RI-ANFIS-3	6
Number of Clusters for RI-ANFIS-4	7
Number of Clusters for RI-ANFIS-5	8
Number of Clusters for RI-ANFIS-6	4
Number of Clusters for RI-ANFIS-7	8
Number of Clusters for RI-ANFIS-8	9
Number of Clusters for RI-ANFIS-9	5
Optimal Value of s	2
$J_s(P(D))_{RI-ANFIS-1}$	0.9921
$J_s(P(D))_{RI-ANFIS-2}$	0.9844
$J_s(P(D))_{RI-ANFIS-3}$	0.9934
$J_s(P(D))_{RI-ANFIS-4}$	0.9932
$J_s(P(D))_{RI-ANFIS-5}$	0.9817
$J_s(P(D))_{RI-ANFIS-6}$	0.9856
$J_s(P(D))_{RI-ANFIS-7}$	0.9884
$J_s(P(D))_{RI-ANFIS-8}$	0.9988
$J_s(P(D))_{RI-ANFIS-9}$	0.9822

8. Closed Loop Performance Analysis

In this section, performance of proposed closed loop fractional order ACP1000 nuclear power plant dynamics and intelligent control is evaluated. The closed loop modelling and control is already proved satisfactory from Fig. 7. The MISO ANFIS controller in LabVIEW in training phase is shown in Fig. 8.

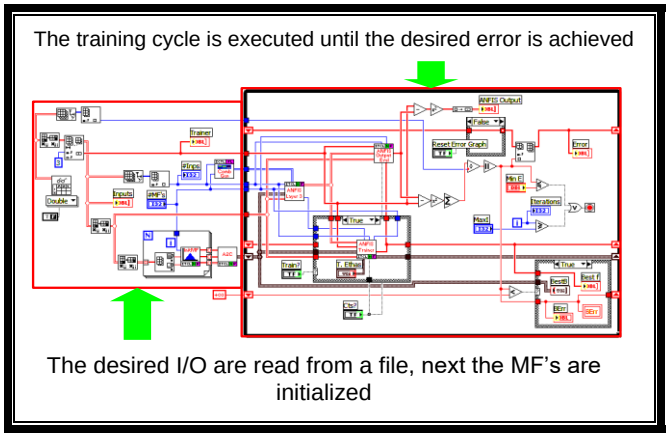

Fig. 8. LabVIEW block diagram code of proposed MISO ANFIS controller in training phase

The optimization of proposed MISO ANFIS pressuriser pressure and level controllers in terms of MSE in closed loop configuration are shown in Fig. 9 and Fig. 10. The mean square error abruptly reduces at around 325 epochs because the closed loop model parameters quickly moving around their stabilized values due to the non-integer nature of model and fast dynamics of neutronic parameters.

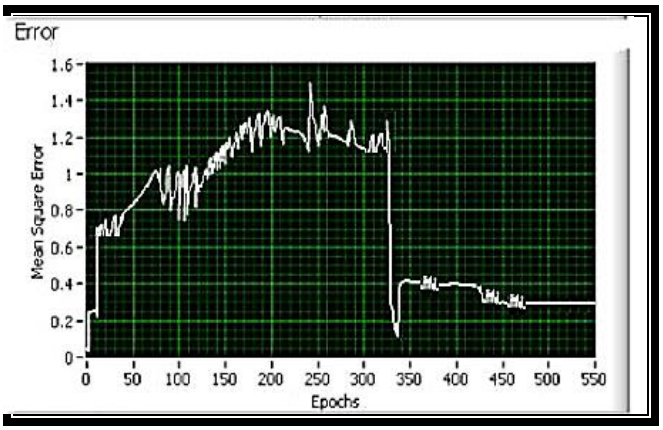

Fig. 9. Optimization of proposed MISO ANFIS pressuriser pressure controller

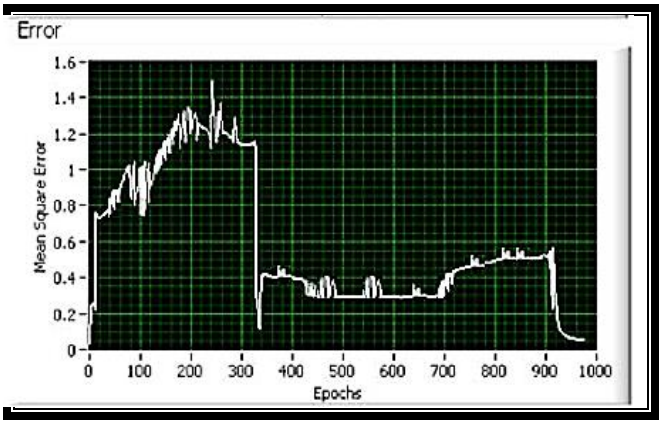

Fig. 10. Optimization of proposed MISO ANFIS pressuriser level controller

Now, some selected parameters of interest are simulated, analysed and validated against benchmark design and operational data of ACP1000 nuclear power plant at 50% steady reactor power [3-5]. The comparison of simulated and benchmark results are tabulated in Table 4.

The power turbine load, reactor neutron flux and power core thermal power, feed water flow & and steam flow and steam generator pressures are shown in Fig. 11 to Fig. 14 respectively.

The scenario is designed for dynamic simulation in which the turbine load is reduced from 100% to 50% at a rate of 10%/min. Optimization of performance was achieved using an increase/reduction of parameters at a rate of 5% /min, whereas, in case study, simulation

experiments were performed at rate of 10% /min in order to prove the robustness of robust intelligent controllers. RI-ANFIS-LV controllers are robust enough to accept the power change rate deviation at a rate of 10% /min specially coupled controlled dynamics of reactor power and turbine power incorporating the primary and secondary systems, dynamics and integrated nature of controllers.

Table 4

Comparison of Simulated and Benchmark Results at 50% Steady Reactor Power

Parameter	Benchmark Value	Simulated Value	Absolute Error
Power Turbine Load (%)	50	50	0
Reactor Neutron Flux (%)	50	50	0
Power Core Thermal Power (%)	50	50	0
Reactor Coolant Pressure (bar)	155	154.95	-0.05
Pressuriser Level (%)	43.5	43.4	-0.1
Average Coolant Temperature (°C)	301.5	301.4	-0.1
Feed Water Flow (t/hr)	1000	998	-2
Steam Flow (t/hr)	1000	998	-2
Steam Pressure (bar)	70.5	70.6	+0.1
Fuel Reactivity (%Δk/k)	0.1	0.095	-0.005
Moderator Reactivity (%Δk/k)	0.15	0.145	-0.005
Control Rod Reactivity (%Δk/k)	-0.25	-0.245	-0.005
Boron Reactivity (%Δk/k)	0	0	0
Total Reactivity (%Δk/k)	0	-0.005	+0.005
Boron Concentration (ppm)	1200	1200	0

The parametric analysis of the simulation experiment presented in Figs. 11 to 14, is now elaborated on time scale from start of transient at zero time prolonged up to 1000 seconds. Firstly; the effect of this power reduction transient is illustrated on primary systems. In the initial 50 seconds of transient, governor valve is closed in effort to decrease the load. The steam pressure is raised in the upstream of governor valve. This increased pressure is exerted pressure back on the inventory of feed water in the steam generator (SG). The increase in pressure is caused coolant saturation temperature to rise slightly, thus the steam production rate (boiling) is decreased, which in turn decrease the heat extraction rate from the reactor coolant system (RCS). Resulting in the rise of cold leg and subsequently hot leg temperature for few seconds. This is caused; the average coolant temperature to raise which directly causes swelling in the primary loop. The increase in volume of RCS is in-surged water into pressuriser thus increasing the pressure of RCS. As the letdown flow rate in PWR is remained constant throughout its operation. The charging flow is adjusted itself by reducing the flow rate. This initial transient is momentary.

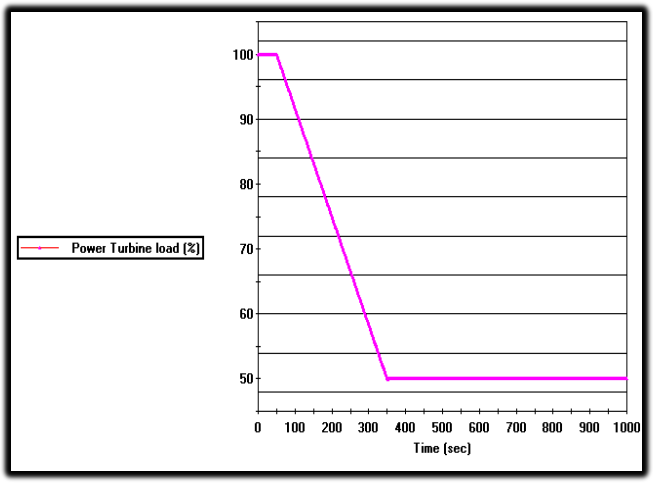

Fig. 11. Dynamics of turbine power load

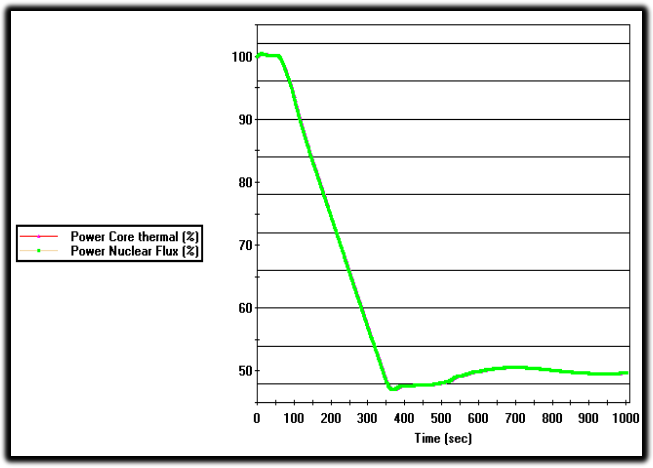

Fig. 12. Dynamics of reactor powers

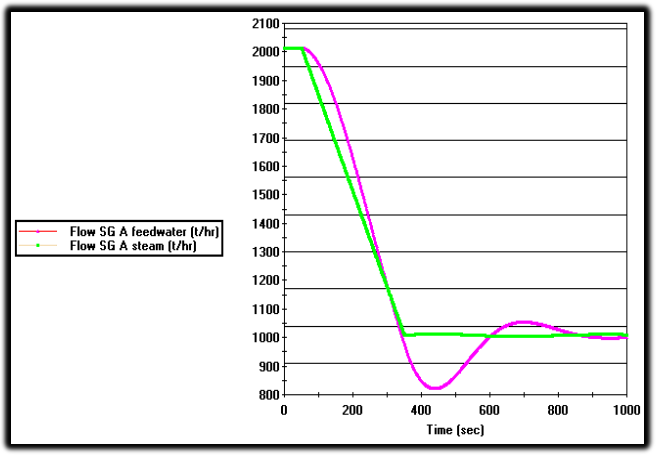

Fig. 13. Dynamics of steam generator flows

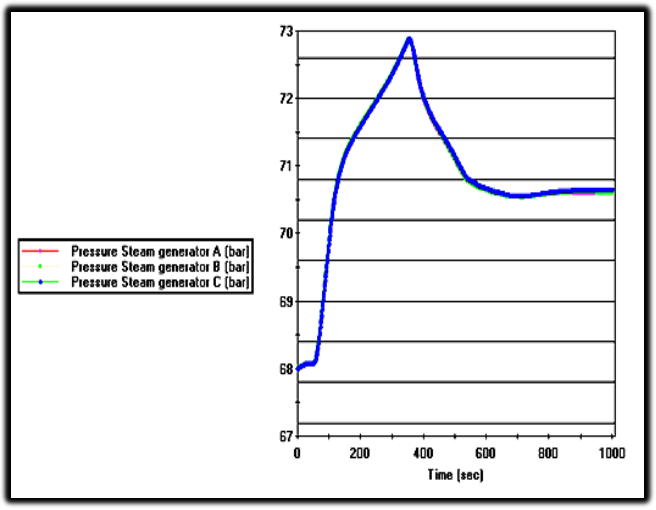

Fig. 14. Dynamics of steam generator pressures

In the next stage from 50 seconds to 350 seconds of transient, the load reduction is started at 50 seconds and is continued at the rate of 10%/min till 350 sec. During this period the plant parameters are monotonically adjusted according to the decreasing load condition.

The load reduction factor stops at 350 seconds and onward, but abrupt decrease in steam generator pressure is seen are around 320 seconds because the feed water flow and steam flow are simultaneously decreasing at a faster rate and cross overlaps at 320 seconds.

Now, from 350 seconds to 1000 seconds of transient, the load rejection process is stopped at 350 seconds, causing transient in plant parameters to converge to normal or new values corresponding to 50% reactor thermal power. During this restoration process, the thermal neutron flux is decreased slightly below 50% due to coarse control of control rods and then recovered to 50%. Since the average coolant temperature is decreased, as a feedback causing the moderator reactivity to rise and to compensate this, control rods are inserted to contribute negative reactivity which causes the overall total negative reactivity, resulting in the decreased neutron flux and subsequently decreased reactor thermal power.

9. Conclusion

A highly nonlinear fractional order complete model of ACP1000 type nuclear power plant has been developed in this research work. The higher order model of the plant has been found very stiff, coupled and multivariable in nature. Primary loop, secondary loop and balance of plant have been extensively modelled. All the differential equations have been realized in modular form using fractional calculus. All the fractional derivatives, integrals and coefficients of models have been optimized in visual basic software. All controllers haven been designed as intelligent ANFIS controllers. Fine tuning of all controllers has been carried out in closed loop configuration in respective MISO and MIMO forms. The process of optimization of controllers' parameters has been accomplished in LabVIEW. A special dedicated interface has been developed between Visual Basic and LabVIEW for model and controller parameters transfer. The performance of the proposed control oriented fractional order ACP1000 simulation model has been evaluated in transient condition and found successful realization based on design data and operational data of ACP1000 nuclear power plant.

10. Acknowledgement

The support of the Pakistan Atomic Energy Commission, Chashma Centre of Nuclear Training and Computer Development Division of KANUPP is gratefully acknowledged.

11. References

[1] F. Cerru, "Preliminary safety report of HPR1000, UKHPR1000GDA Project, Report HPR/GDA/PSR", International Atomic Energy Agency, 2017.

[2] T. Xin, "Safety Approach and Safety Assessment, Hualong HPR1000, IFNEC Report", International Atomic Energy Agency, 2018.

[3] L. C. C. Po, and J. M. Link, "PCTRAN-3 / U 3-LP", Micro-Simulation Technology, vol. 38, pp. 1-27, 2018.

[4] M. Zirong and Y. Zenghua, "Improvement of M310 PWR Study on the Load Follow Without Boron Adjustment", Chinese Journal of Nuclear Science and Engineering, vol. 24, no. 4, pp. 294-300, 2018.

[5] B. Lan, Q. Meng, J. Yang and Y. Cai, “Analysis and Application of Load Change Rate Algorithm for CPR1000 Nuclear Power Plant”, Journal of Nuclear Power Engineering, vol. 38, No. 4, pp. 51-55, 2017.

[6] C. Fazekas, G. Szederkenyi and K. M. Hangos, "A Simple Dynamic Model of the Primary Circuit in VVER Plants for Controller Design Purposes", Nuclear Engineering and Design, vol. 237, no. 10, pp. 1071-1087, 2007.

[7] H. Xie, H. Gu, C. Lu and J. Ping, "Online Simulation of nuclear Power Plant Primary Systems", Science and Technology of Nuclear Installations, vol. 20, pp. 1-9, 2020.

[8] W. Sun, D. Liu, J. Zhao and F. Dong, “An AP1000 Nuclear Power Plant Dynamic Model Suitable for Stability Analysis of Power Grid”, Power System Technology, vol. 27, no. 2, pp. 181-192, 2014.

[9] J. Zhang, S. S. Yin, L. Chen, Y. C. Ma, M. J. Wang, H. Fu, Y. W. Wu, W. X. Tian, S. Z. Qiu and G. H. Su, “A Study on the Dynamic Characteristics of Secondary Loop in Nuclear Power Plant”, Nuclear Engineering and Technology, vol. 20, pp. 1-9, 2020.

[10] C. I. Muresan, C. Copot, C. Ionescu and R. D. Keyser, “Robust Fractional Order Control of LPV Dynamic Mechatronic Systems”, IEEE 15th International Conference on Control and Automation, pp. 154-159, 2019.

[11] A. Takeshita, T. Yamashita, N. Kawaguchi and M. Kuroda, “Fractional Order LQR and State Observer for a Fractional Order Vibratory System”, Journal of Applied Sciences, vol. 1, pp. 1-20, 2021.

[12] M. Ghorbani, “Robust Stability Analysis of Interval Fractional-Order Plants by Fractional Order Controllers”, International Journal of General Systems, vol. 50, no. 1, pp. 1-25, 2020.

[13] G. E. Paredes, “Fractional Space Neutron Point Kinetics (F-SNPK) Equations for Nuclear Reactor Dynamics”, Annals of Nuclear Energy, vol.107, pp. 136-143, 2016.

[14] M. Zarei, “A Reflection on the Fractional Order Nuclear Reactor Dynamics”, Applied Mathematical Modelling, vol. 73, pp. 349-364, 2019.

[15] S. Mehta, K. Vasoya and D. Adhyaru, “ANFIS as a Controller for Fractional Order System”, 5th Nirma University International Conference on Engineering, Ahmedabad, India, IEEE, pp. 1-5, 2015.

[16] S. A. Saadat, S. M. Ghamari, H. Mollaee and F. Khavari, “Adaptive Neuro-Fuzzy Inference Systems (ANFIS) Controller Design on a Single Phase Full Bridge Inverter with a Cascade Fractional Order PID Voltage Controller”, The Institution of Engineering and Technology, vol. 14, no. 11, pp. 1960-1972, 2021.

[17] B. Selma, S. Chouraqui and H. Abouaissa, “Optimization of ANFIS Controllers using Improved Ant Colony to Control an UAV Trajectory Tracking Task”, SN Applied Sciences, vol. 20, no. 2, pp. 1-18, 2020.

[18] C. Yeom and K. Kwak, “Performance Comparison of ANFIS Models by Input Space Partitioning Methods”, Symmetry, vol. 18, no. 10, pp. 1-25, 2018.

